MASS PARTICIPATION IN NON-CLASSICAL MASS ISOLATED SYSTEMS

M. Ziyaeifar[*] and Sh. Tavousi
International Institute of Earthquake Engineering and Seismology
No.26, Arghavan Street, Dibaji, Farmanieh, 19531, Tehran, Iran.

ABSTRACT

Application of new techniques in seismic design of structures is usually accompanied with the use of large capacity energy dissipation devices in the system. In such cases, the assumption of classical (proportional) damping is not usually valid and non-classical features prevail in the system. Non-classical behavior is a known subject in dynamics of structures and the required mathematical basis to address different aspects of such systems is readily available in the literature. In the context of system characteristics, however, the role and the significance of each mode in total response of these structure, subjected to earthquake excitation, has not yet been properly communicated among the researchers. This study offers an intuitive adaptation for mass participation factor of non-classical systems to signify the modal contribution role of non-classical mass isolated buildings. The proposed factor is useful in determining the importance of isolated modes of such systems and speculating on the general behavior of these structures. A spectrum analysis technique for non-classical systems is also projected in this study. Reliability of the definition for mass participation factor in this study is verified through some numerical examples. A supplementary conclusion suggests limiting the use of classical analytical tools in analysis of mass isolated systems to the structures with low damping ratios.

Keywords: mass isolation, mass participation factor, non-classical systems

1. INTRODUCTION

Most of the new techniques in seismic design of structures are based on changing the dynamic characteristics of buildings to receive less earthquake input force and energy and to dissipate the energy with lower damage and deformation in structural components of the system. These techniques usually transfer the first natural period of the structure to the zone of low input energy and force of earthquake spectrum by increasing the flexibility of the system. This, in turn, improves the energy dissipation potential of the system by providing larger relative deformations in the structure.

---

[*] E-mail address of the corresponding author: ziyaeifar@msn.com

Most of these techniques are using viscous devices to dissipate earthquake input energy in the system and to reduce seismic effects on structural components of building. Among them, Base Isolation is a well known technique due to its phenomenal potential in reducing earthquake effects in buildings. This technique elongates the natural period of the first mode of the system and increases its damping ratio and mass participation factor [1]. In spite of some similarities with base isolation, other approaches are known, mostly, as damping enhancement techniques for structures subjected to earthquakes.

Mass isolation is a notion that has been proposed to clarify the concept of vibration isolation in the case of seismic excitation [2, 3]. Using this viewpoint, the efficiency of a majority of new techniques in vibration isolation can be evaluated based on the shift in natural period, damping ratio and mass participation factor of first few modes of the system. According to this concept, base isolation is a superior approach, not only because of its ability to shift the natural period of the system but due to its remarkable potential in shifting the mass participation factor of the first mode of the structure (this factor in base isolation is shifted close to 100% for highly-flexible, low-damp linear-isolators [4,1]).

Existence of high capacity viscous devices in Multi-degrees of freedom systems may cause the assumption of proportionality of damping matrix with mass and stiffness matrices to be unacceptable. In this case such systems should be categorized as non-classical structures and their un-damped dynamic characteristics (derived based on mass and stiffness matrices) can not be trusted as the true characteristics of the system (e.g. natural periods, modal shapes, and mass participation factors). In mass isolation viewpoint, using such unreliable characteristics may cause improper efficiency evaluation for mass isolation and it was recommended to use damped characteristics of the system in appraising isolation efficiency of such structures [3].

Although mathematical basis for determining natural periods, modal shapes and damping ratios of non-classical systems is readily available [5, 6], there is hardly any clue in the literature, addressing a technique to calculate mass participation factor for non-classical systems.

Due to the importance of mass participation factor in evaluation of mass isolated systems, the focus of the current study is to find a method in estimation of mass participation factor for non-classical systems. Besides, it is also attempted to expand a spectrum analysis technique for non-classical systems to be able to have a simple approach in determination of response of such structures. Furthermore, it is also intended to investigate the accuracy of classical techniques in analysis of non-classical systems and to come up to some preliminary perception in limiting the application of such techniques in mass isolated buildings.

2. NON-CLASSICAL SYSTEMS AND MASS ISOLATION

In general, if descriptive matrices of a multi degrees of freedom system do not represent the property shown in the following relationship; the structure is known, theoretically, as a non-classical system [7].

$$[C]\,[M]^{-1}\,[K]=[K]\,[M]^{-1}\,[C] \tag{1}$$

In which [C], [M] and [K] are damping, mass and stiffness matrices, respectively. Definition of classical systems based on proportionality of damping matrix with stiffness and/or mass matrices can be inferred from the above relationship.

If damping capacity of a non-classical system is small, the assumption of classical behavior is usually acceptable. In reality, this is the case for most of the ordinary structures with small damping ratios. In the case of large damping capacity, well distribution of this capacity in the structure may cause a kind of ad hoc proportionality of damping matrix with mass or stiffness matrices, providing the chance of using the assumption of classical behavior without accepting large inaccuracies. This issue will be addressed later in this study. However, when large damping capacity in the form of few concentrated viscous dashpots exists in the structure, the assumption of classical behavior may no longer be valid. This would be the case, particularly, if distribution of damping capacity presents no (or little) similarities with mass and stiffness distribution across the system. Mass Isolation techniques are mostly fit into this group of structures. Figure 1 shows some of these techniques (see, Ref. [3]). Methods b, c and e shown in figure are set to have large damping capacity in the form of few concentrated viscous devices, causing explicit non-classical characteristics for each class of these structural systems.
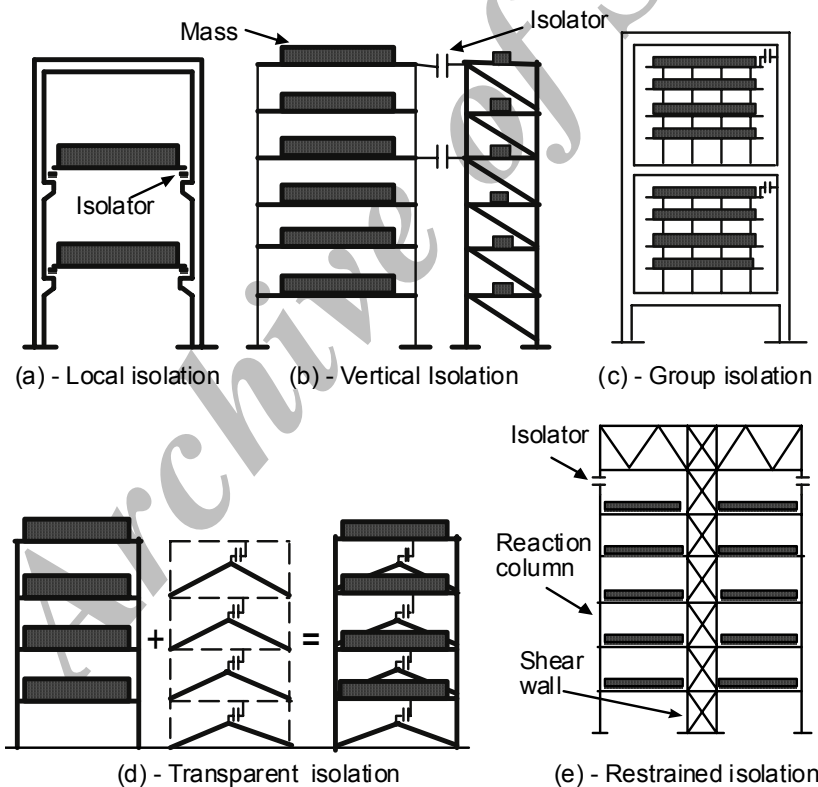

Figure 1. Methods of Mass Isolation

In non-classical systems, characteristic equations incorporates damping matrix besides

the usual mass and stiffness matrices in classical systems. Solving this set of equations results in natural frequencies, modal shapes and damping ratios of all modes of the system. Having a mathematical representation for damping ratio of all modes is an important feature of non-classical modal analysis of structures (in classical modal analysis, except approximation, there is no mathematical basis for calculation of damping ratios). Another important aspect of non-classical modal analysis is the modal shapes of the structure that, in contrast with classical systems, are consisted of real and imaginary components (see, for example, [5] and [6]).

Having all these, participation potential of mode shapes in response of the system (subjected to earthquake excitation) is still unclear. In classical systems there is an indication for such issue that is called Mass Participation Factor (hereinafter MPF) [8]:

$$\alpha_C^j = \frac{1}{M} \cdot \frac{L_j^2}{M_j} \tag{2}$$

In which, M is total mass of the system, M_j is generalized modal mass for the jth mode and L_j is modal earthquake participation factor. Mass participation factor α_C^j, can be interpreted as the ratio of total mass that acts in mode j and generates the share of that mode from total base shear, i.e.

$$vs(t) = \sum_{j=1}^{n}(\alpha_C^j M).P_j V_j(t) = \sum_{j=1}^{n}(M_C^j).P_j V_j(t) \tag{3}$$

In this equation, $vs(t)$ is total base shear (time history), P_j is natural frequency of each mode and $V_j(t)$ is earthquake response integral for each particular mode. The later is known, usually, as the instantaneous pseudo velocity function. Parameter $M_C^j = L_j^2/M_j$ is the allocated mass for the jth mode (subscript C stands for classical systems) and it is called the effective modal mass.

Mass participation factor, may not be considered as a dependable measure for representing the importance of each mode. This is due to the fact that, frequency contents of input earthquakes could cause any particular mode to have an unexpected level of contribution in response of the system (base shear is governed by both $P_j V_j(t)$ and $\alpha_C^j M$ terms). In mass isolated systems, however, MPF has a conceptual significance. In such systems the level of isolation realization can be simply measured by the potential of each isolation technique in removing higher mode effects from the response of the system (higher modes are positioned in the high energy zone of earthquake spectrum and requiring large force and deformations in the structural components). For example, in a base isolated system, ideally, there is only one isolated mode (in the low energy zone of earthquake spectrum) and higher modes are supposedly eliminated (theoretically $\alpha_C^1 \cong 1.$ and $\alpha_C^2 \cdots \alpha_C^n \cong 0.$). Accordingly, in mass isolated systems MPF is a parameter that shows if a major part of the mass of building has been actually isolated and if a significant

contribution of higher modes in response of the structure would be expected.

3. MASS PARTICIPATION FACTOR FOR NON-CLASSICAL SYSTEMS

To put forward the concept of mass participation factor for non-classical systems, the same approach used for MPF derivation in classical systems is basically followed [8]. The process starts with calculation of elastic forces using modal displacement vector.

$$\{f(t)\} = [K]\{x(t)\} \tag{4}$$

In which $\{x(t)\}$ is time history displacement vector of the system. In non-classical structures displacement vector $\{x(t)\}$ can be written as:

$$\{x(t)\} = 2\sum_{j=1}^{n} \text{Re}\left[B_j\{\Psi_j\} v_0 e^{r_j t}\right] \tag{5}$$

In which n is the number of modes and B_j is modal participation factor for the velocity change v_0. Ψ_j and r_j are characteristic vector and characteristic value of non-classical systems. The above relationship is directly quoted from the work of Veletsos et al. [9]. To be consistent with the literature and to improve the readability of the text, the same notations and derivation techniques introduced in the above mentioned work are used in development of the current subject. Substitution of Eq. (5) into Eq. (4) results in the following relationship.

$$\{f(t)\} = 2\sum_{j=1}^{n} \text{Re}\left[[K]\{\Psi_j\} B_j v_0 e^{r_j t}\right] \tag{6}$$

Similar to the process used in classical systems, modal characteristic equation, shown below, is used to replace the stiffness matrix in the above equation.

$$[K]\{\Psi_j\} = -r_j^2[M]\{\Psi_j\} - r_j[C]\{\Psi_j\} \tag{7}$$

Considering,

$$r_j = -\xi_j P_j + i\hat{P}_j \qquad \text{and} \qquad \hat{P}_j = P_j\sqrt{(1-\xi_j^2)}$$

Where, ξ_j, P_j and $\hat{P}_j$ are damping ratio, natural frequency and damped frequency of each mode, respectively. Characteristic equation is further expanded and substitute in Eq. (6) as follows.

$$\{f(t)\} = 2 \sum_{j=1}^{n} Re\left[\begin{pmatrix} P_j^2[M] - 2\xi_j^2 P_j^2[M] + \xi_j P_j[C] + \\ 2i\xi_j P_j^2 \sqrt{(1-\xi_j^2)}[M] - iP_j\sqrt{(1-\xi_j^2)}[C] \end{pmatrix}\{\Psi_j\}B_j e^{r_j t}\right]v_0 \qquad (8)$$

Furthermore, the following complex vector partitioning, proposed by Veletsos et al [9], is used to simplify the above formula.

$$2B_j\{\Psi_j\} = \{\beta_j^v\} + i\{\gamma_j^v\}$$

By substituting the above relationship into Eq. (8) and following some algebraic operations (similar to those in Ref. [9]), we will have:

$$\{f(t)\} = \sum_{j=1}^{n} e^{-\xi_j P_j t}\left[\begin{matrix} (\{\beta_j^v\}\cos \hat{P}_j t - \{\gamma_j^v\}\sin \hat{P}_j t)\left(P_j^2[M] - 2\xi_j^2 P_j^2[M] + \xi_j P_j[C]\right) + \\ (\{\beta_j^v\}\sin \hat{P}_j t + \{\gamma_j^v\}\cos \hat{P}_j t)\left(P_j\sqrt{(1-\xi_j^2)}[C] - 2\xi_j P_j^2 \sqrt{(1-\xi_j^2)}[M]\right) \end{matrix}\right]v_0 \qquad (9)$$

Response of a single degree of freedom damped system subjected to unit velocity change can be written as:

$$h_j(t) = \frac{1}{\hat{P}_j} e^{-\xi_j P_j t} \sin \hat{P}_j t \quad \text{and} \quad \dot{h}_j(t) = e^{-\xi_j P_j t}\left[\cos \hat{P}_j t - \frac{\xi_j}{\sqrt{1-\xi_j^2}} \sin \hat{P}_j t\right] \qquad (10)$$

Where $h_j(t)$ and $\dot{h}_j(t)$ are displacement and velocity time histories, respectively. Using the above relationships, trigonometric terms in Eq. (9) are replaced with $h_j(t)$ and $\dot{h}_j(t)$.

$$\{f(t)\} = \sum_{j=1}^{n}\left[\begin{matrix} \left(P_j^2[M] - 2\xi_j^2 P_j^2[M] + \xi_j P_j[C]\right)\left(\{\alpha_j^v\}P_j h_j(t) + \{\beta_j^v\}\dot{h}_j(t)\right) + \\ \left(P_j\sqrt{(1-\xi_j^2)}[C] - 2\xi_j P_j^2\sqrt{(1-\xi_j^2)}[M]\right)\left(\{\omega_j^v\}P_j h_j(t) + \{\gamma_j^v\}\dot{h}_j(t)\right) \end{matrix}\right]v_0 \qquad (11)$$

In which,

$$\{\alpha_j^v\} = \xi_j\{\beta_j^v\} - \sqrt{(1-\xi_j^2)}\{\gamma_j^v\} \quad \text{and} \quad \{\omega_j^v\} = \xi_j\{\gamma_j^v\} + \sqrt{(1-\xi_j^2)}\{\beta_j^v\}$$

To find the time history response of the structure subjected to earthquake excitation, the velocity change (v_0) during time increment $d\tau$ is substitute by $v_0 = v(\tau) = -\ddot{x}_g(\tau)\,d\tau$ in which $\ddot{x}_g(\tau)$ is base acceleration at time $t=\tau$. The change in elastic force during this time increment (at $t \rangle \tau$) is written as:

$$\{df\} = -\sum_{j=1}^{n}\left[\begin{array}{l}\left(P_j^2[M]-2\xi_j^2 P_j^2[M]+\xi_j P_j[C]\right)\left(\{\alpha_j^v\}P_j h_j(t-\tau)+\{\beta_j^v\}\dot{h}_j(t-\tau)\right)+\\\left(P_j\sqrt{(1-\xi_j^2)}[C]-2\xi_j P_j^2\sqrt{(1-\xi_j^2)}[M]\right)\left(\{\omega_j^v\}P_j h_j(t-\tau)+\{\gamma_j^v\}\dot{h}_j(t-\tau)\right)\end{array}\right]\ddot{x}_g(\tau)d\tau \quad (12)$$

By integration over the time domain ($o \le \tau \le t$) elastic force at time *t* would be:

$$\{f(t)\} = \sum_{j=1}^{n}\left[\begin{array}{l}\left(P_j[M]-2\xi_j^2 P_j[M]+\xi_j[C]\right)\left(\{\alpha_j^v\}P_j V_j(t)+\{\beta_j^v\}P_j\dot{D}_j(t)\right)+\\\left(\sqrt{(1-\xi_j^2)}[C]-2\xi_j P_j\sqrt{(1-\xi_j^2)}[M]\right)\left(\{\omega_j^v\}P_j V_j(t)+\{\gamma_j^v\}P_j\dot{D}_j(t)\right)\end{array}\right] \quad (13)$$

In which $V_j(t)$ and $\dot{D}_j(t)$ are time history functions known as instantaneous pseudo velocity and relative velocity response of single degree of freedom systems, respectively. These functions are represented by the following expressions.

$$V_j(t) = -p_j\int_0^t\ddot{x}_g(\tau)\,h_j(t-\tau)d\tau \quad \text{and} \quad \dot{D}_j(t) = -\int_0^t\ddot{x}_g(\tau)\,\dot{h}_j(t-\tau)\,d\tau \quad (14)$$

Equation 13 after simplification is written as:

$$\{f(t)\} = \sum_{j=1}^{n}\left[\begin{array}{l}\left([MC]_j^A\right)\left(\{\alpha_j^v\}P_j V_j(t)+\{\beta_j^v\}P_j\dot{D}_j(t)\right)+\\\left([MC]_j^B\right)\left(\{\omega_j^v\}P_j V_j(t)+\{\gamma_j^v\}P_j\dot{D}_j(t)\right)\end{array}\right] \quad (15)$$

Where $[MC]_j^A$ and $[MC]_j^B$ are summation of matrices in the first and the second terms of Eq. (13). Further simplification results in the following relationship.

$$\{f(t)\} = \sum_{j=1}^{n}\left(\{\alpha_{MC}^j\}+\{\omega_{MC}^j\}\right)P_j V_j(t) + \sum_{j=1}^{n}\left(\{\beta_{MC}^j\}+\{\gamma_{MC}^j\}\right)P_j\dot{D}_j(t) \quad (16)$$

The subsequent expressions are used in the above simplification.

$$[MC]_j^A \times \{\alpha_j^v\} = \{\alpha_{MC}^j\}$$
$$[MC]_j^B \times \{\omega_j^v\} = \{\omega_{MC}^j\}$$
$$[MC]_j^A \times \{\beta_j^v\} = \{\beta_{MC}^j\}$$
$$[MC]_j^B \times \{\gamma_j^v\} = \{\gamma_{MC}^j\}$$

The next step is to calculate the base shear by adding together lateral forces along the height. This is accomplished by pre-multiplication of a unit vector in Eq. (16).

$$vs(t) = \langle 1 \rangle \{ f(t) \} = \sum_{j=1}^{n} \left[\left(\alpha_{MC}^{j} + \omega_{MC}^{j} \right) P_j V_j(t) + \left(\beta_{MC}^{j} + \gamma_{MC}^{j} \right) P_j \dot{D}_j(t) \right] \qquad (17)$$

In which:

$$\alpha_{MC}^{j} = \langle 1 \rangle \{ \alpha_{MC}^{j} \}$$
$$\omega_{MC}^{j} = \langle 1 \rangle \{ \omega_{MC}^{j} \}$$
$$\beta_{MC}^{j} = \langle 1 \rangle \{ \beta_{MC}^{j} \} \quad \gamma_{MC}^{j} = \langle 1 \rangle \{ \gamma_{MC}^{j} \}$$

Now Eq. (17) can be rewritten as:

$$vs(t) = \sum_{j=1}^{n} \left[(\alpha\omega_{MC}^{j}) P_j V_j(t) + (\beta\gamma_{MC}^{j}) P_j \dot{D}_j(t) \right] \qquad (18)$$

Where,

$$\alpha\omega_{MC}^{j} = \alpha_{MC}^{j} + \omega_{MC}^{j} \quad \text{and} \quad \beta\gamma_{MC}^{j} = \beta_{MC}^{j} + \gamma_{MC}^{j}$$

A similarity between the above equation and Eq. (3) can be distinguished. In contrast with classical systems, base shear in non-classical structures consists of two different components. The first one is similar to the base shear definition in classical system Eq. (3) and is composed of a factor ($\alpha\omega_{MC}^{j}$) with dimension of mass and a time varying function ($P_j V_j(t)$) with the dimension of acceleration. The second component resembles the first one but, instead of pseudo-velocity ($V_j(t)$) it contains the relative velocity ($\dot{D}_j(t)$) term. Both $\alpha\omega_{MC}^{j}$ and $\beta\gamma_{MC}^{j}$ factors have the dimension of mass and, apparently, MPF should be a combination of them. This conclusion suggests a relationship between $V_j(t)$ and $\dot{D}_j(t)$ functions to be found. However, since mass participation factor is considered a system characteristic, it should not be dependable on earthquake excitation parameters such as pseudo-velocity and relative velocity relationship. Ironically, it seems, without such relationship MPF for non-classical systems does not exist.

After all, the main challenge in finding MPF for non-classical systems seems to be the dilemma that puzzled many researchers so far. Finding a relationship between pseudo-velocity and relative velocity in the time domain might have not been the case since $V_j(t)$ and $\dot{D}_j(t)$ are functions with asymmetrical characteristics. Nevertheless, literature shows distinct viewpoints in finding relationships between maximum values of these functions (in dealing with spectral analysis of non-classical systems). Following these footsteps, in this work at first a relationship between maximum values of the above time functions (applicable to a wide range of earthquakes) is introduced. Later, using this relationship in a spectral approach, relative velocity is replaced with the pseudo-velocity term. At last, the assumption of stationary process is used and two unsynchronized terms are put together and an approximation for MPF in non-classical systems is obtained.

3.1 Pseudo-velocity versus relative velocity
Using two spectrums for pseudo-velocity and relative velocity in spectral analysis of non-classical systems is not desirable and different approaches have been proposed to simplify this procedure (see, for example, Gupta [10] and Igusa et al. [11]). It seems that the first step for a rational approach in this case is to know how the two spectrums relate to each other. One of the recent works in this area is reported by Pekan et al. [12], where some relationships based on natural frequency and damping ratios are proposed to correlate the maximum values of the two velocity functions. In this study, to ease the correlation procedure, the relationships proposed by Pekan et al. are condensed out, after broad simplification, into the following compact formula.

$$\eta = f(\xi, T) = 0.8 - 0.6\xi + 0.17T + 0.4\xi\,T \quad \text{where,} \quad \dot{D}\,(t)\Big|_{Max} = \eta\,V\,(t)\Big|_{Max} \quad (19)$$

In which η is the correlation coefficient, T is period (in Sec.) and ξ is damping ratio. Figure. 2 compares the correlation coefficient obtained from the above formula with those of the Pekan's relationships in two different levels of damping ratios. As shown in figure, the proposed formula is in close agreement with the Pekan's relationships. It should be noted that, the above formula (as well as the Pekan's relationships) is checked only for damping ratios less or around 0.5 (i.e. $\xi \leq 0.5$) but this limitation is not followed in here and the same formula is applied for higher damping ratios (till $\xi \leq 0.9$).
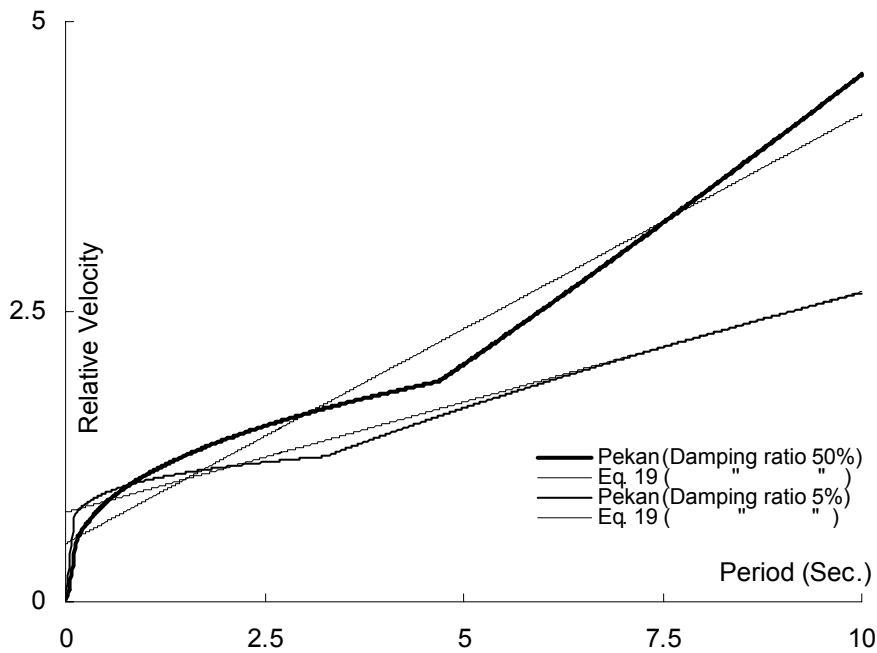

Figure 2. Relative Velocity vs. Pseudo Velocity

3.2 Mass participation factor in terms of maximum value of base shear
Using Eq. (18), the share of each mode from total base shear is written as:

$$vs(t)_j = (\alpha\omega_{MC}^j)P_jV_j(t) + (\beta\gamma_{MC}^j)P_j\dot{D}_j(t) \tag{20}$$

Based on the assumption of stationary random process, maximum value of the above formula can be obtained using the SRSS[1] approach (see, Der Kiureghian [13]).

$$vs(t)_j\big|_{Max} = \sqrt{\left((\alpha\omega_{MC}^j)P_jV_j(t)\big|_{Max}\right)^2 + \left((\beta\gamma_{MC}^j)P_j\dot{D}_j(t)\big|_{Max}\right)^2} \tag{21}$$

By using Eq. (19) we will have:

$$vs(t)_j\big|_{Max} = \sqrt{(\alpha\omega_{MC}^j)^2 + \eta_j^2(\beta\gamma_{MC}^j)^2}\ \ P_jV_j(t)\big|_{Max} \tag{22}$$

The square root term in the above equation is called, hereinafter, Effective Modal Mass for non-classical systems, i.e.

$$vs(t)_j\big|_{Max} = M_{NC}^j\ P_jV_j(t)\big|_{Max} \quad \text{where} \quad M_{NC}^j = \sqrt{(\alpha\omega_{MC}^j)^2 + \eta_j^2(\beta\gamma_{MC}^j)^2} \tag{23}$$

Thus, mass participation factor for non-classical systems is defined as:

$$\alpha_{NC}^j = \frac{M_{NC}^j}{M_{NC}} \quad \text{in which} \quad M_{NC} = \sum_{j=1}^n M_{NC}^j \tag{24}$$

M_{NC} in the above equation is total effective mass of the system that, in contrast with classical systems, may not be equivalent to the real mass of the structure (M). Furthermore, total Maximum base shear using SRSS approach would be as follows.

$$vs(t)\big|_{Max} = \sqrt{\sum_{j=1}^n (\alpha_{NC}^j M_{NC}\ P_jV_j(t)\big|_{Max})^2} \tag{25}$$

In classical systems an identical equation for maximum base shear exists, in which, $\alpha_C^j M$ simply replaces the term $\alpha_{NC}^j M_{NC}$ in the above expression [8].

To be correct, the proposed expression for mass participation factor (α_{NC}^j in Eq. (24)) is not literally similar to the one for classical systems (α_C^j in Eq. (2)). In fact α_{NC}^j is obtained based on maximum values of base shear while α_C^j is not related to whatever expression

---

1- Square Root of the Sum of Squares

used for the base shear (maximum values or time history). Also, using η_j in defining α_{NC}^j means dependency of mass participation factor to the characteristics of input earthquakes (considering that α_C^j is not related to any earthquake parameters). Moreover, α_{NC}^j is not a real system characteristic because η_j is a direct function of other characteristics of the system (ξ_j and T_j). In other words, α_{NC}^j is a make up figure that may not compellingly posses the specific features required for a system characteristic. Nevertheless, the proximity of α_{NC}^j definition to the MPF envisage in non-classical systems will be shown later in this study.

3.3 MPF in the time domain
α_{NC}^j definition in this study is considered a weak adaptation for MPF in non-classical systems. Hypothetically, an ideal MPF for non-classical systems (if exists) should comply with the following expression.

$$vs(t) = \sum_{j=1}^{n} (\overline{\alpha}_{NC}^j \overline{M}_{NC}).P_j \overline{V}_j(t) \tag{26}$$

In which $\overline{\alpha}_{NC}^j$ is the speculated non-classical MPF defined in the time domain. $\overline{M}_{NC}$ and $\overline{V}_j(t)$ are the appropriate effective mass and velocity function for the above MPF, respectively. In the case of existence of such MPF, Eq. (26) would be equivalent to Eq. (18). Now the question is, what it takes if we use the previous MPF derived based on maximum values of base shear (α_{NC}^j) and its counterparts M_{NC} and $V_j(t)$ in the time history relationship Eq. (26) instead of hypothetically correct parameters $\overline{\alpha}_{NC}^j$, $\overline{M}_{NC}$ and $\overline{V}_j(t)$. To answer this question derivation is pursued from another viewpoint.

Let's start by scaling the amplitude of pseudo-velocity function (using parameter η_j in Eq. (19)), so that, its maximum value to be equivalent to the maximum valve of relative velocity function.

$$\dot{D}_j(t) \approx \eta_j V_j(t) \big\|^{\text{Max. Scaled}} \tag{27}$$

The two functions $\eta_j V_j(t)$ and $\dot{D}_j(t)$ are equivalent only base on their maximum amplitudes and substitution of scaled pseudo velocity term instead of relative velocity in Eq. (20) would not be possible, i.e.

$$vs(t)_j \neq (\alpha \omega_{MC}^j) P_j V_j(t) + (\beta \gamma_{MC}^j) P_j \eta_j V(t) \tag{28}$$

Supposing that, SRSS technique can be applied to each time increment of the above

inequality (a wrong assumption, in fact) to find instantaneous time history resultant of the above terms.

$$\text{vs(t)}_j \approx \sqrt{(\alpha\omega_{MC}^j)^2 + \eta_j^2\,(\beta\gamma_{MC}^j)^2}\ P_j V_j(t)\quad = M_{NC}^j\ P_j V_j(t) \qquad (29)$$

In which M_{NC}^j is the same effective modal mass for non-classical systems (obtained before in Eq. (23)). Subsequently:

$$\text{vs(t)} \approx \sum_{j=1}^{n}\alpha_{NC}^j\ M_{NC}\ P_j V_j(t) \qquad (30)$$

α_{NC}^j is also the same mass participation factor introduced in Eq. (24). According to the above relationship mass participation factor based on maximum values, α_{NC}^j , can serve as an approximation for $\overline{\alpha}_{NC}^{\,j}$ (hypothetically exact MPF) if SRSS concept extends, inappropriately, to each instance of the process. Accuracy of α_{NC}^j definition in the time domain (i.e. Eq. (30)) will be addressed later in this study.

4. SPECTRAL ANALYSIS IN NON-CLASSICAL SYSTEMS

Spectral methods in earthquake engineering are known for their simplicity in the analysis procedure. However, these techniques in non-classical systems are still unsettled and a rational approach bringing together the alleged simplicity with the required accuracy is yet to be found.

Since response of non-classical systems usually consists of two different terms (similar to those in Eq. (18) for base shear), in spectral approach they are requiring two types of spectrums (e.g. pseudo and relative velocity spectrums). For simplicity, some researchers use the equivalency assumption for the two spectrums (Villaverde [14] and Sinha et al.[15]). Introduction of Eq. (19), however, provides the ground for a sensible approach in non-classical spectral analysis by simplification of the relationship between the two spectrums without broadly compromising on the accuracy of the analysis.

This viewpoint is shown, beforehand, in Eq. (25) which is, in fact, a spectral evaluation for base shear using ordinary pseudo-velocity spectrum. This equation can now be written in a more familiar form.

$$\text{vs(t)}\big|_{Max} = \sqrt{\sum_{j=1}^{n}\Big(\text{vs(t)}_j\big|_{Max}\Big)^2}\quad \text{where}\quad \text{vs(t)}_j\big|_{Max} = \alpha_{NC}^j\,M_{NC}\,P_j\,psv(\omega_j,\xi_j) \qquad (31)$$

In which $psv(\omega_j,\xi_j)$ is the spectral pseudo-velocity term. The simple algebra that provides the relationship for base shear response of the system (in the form of Eq. (18)) can also be followed for other responses of non-classical systems. For example, time history

displacement response of such systems is known as [9]:

$$\{x(t)\} = \sum_{j=1}^{n} \left[\{\alpha_j^v\} V_j(t) + \{\beta_j^v\} \dot{D}_j(t) \right] \tag{32}$$

All terms in the above relationship have been previously defined (note that, dimensions of the vectors $\{\alpha_j^v\}$ and $\{\beta_j^v\}$ are time per radian). Using the same procedure for base shear, spectral analysis for maximum modal displacements results in the following relationship.

$$\begin{cases} \{x(t)_j\}_{Max} = \{\lambda_j\} V_j(t)\big|_{Max} \\ \\ \text{where} \quad \{\lambda_j\} = \sqrt{\{\alpha_j^v\}^2 + \eta_j^2 \{\beta_j^v\}^2} \end{cases} \Rightarrow \{x(t)_j\}_{Max} = \{\lambda_j\} psv(\omega_j, \xi_j) \tag{33}$$

The above approach in spectral analysis of non-classical systems presents both simplicity and accuracy in the analysis procedure. In non-classical systems with large coefficient for the relative velocity term (e.g. $\{\beta_j^v\}$ in Eq. (32) or $\beta\gamma_{MC}^j$ in Eq. (18)) accuracy of this technique would be more pronounced. In addition, since high damping ratios and long natural periods considerably increase the value of η (see Figure.2), accuracy of the above spectral approach in such cases will be higher than those without a proper relationship between the two spectrums.

5. VERIFICATION OF MPF FOR NON-CLASSICAL SYSTEMS

A computer code has been developed to examine the dependability of the so-called mass participation factor for non-classical systems. Program is capable of calculating time history responses of shear type structures (displacement, lateral force and base shear using Eq. (32), 16 and 18, respectively). It also determines mass participation factor for non-classical systems (α_{NC}^j using Eq. (24)) and the spectral values for base shear (Eq. (25) or (31)). In addition, the program also computes another time history response for the base shear using Eq. (30) (approximated time history response based on MPF definition).

Two examples for numerical investigation are used in this study (illustrated in Figure 3). Both examples (St-A and St-B) are from a class of mass isolated systems that is called Vertical Isolation (shown in Figure.1-b). In mass isolation viewpoint, as described elsewhere [3], isolated structures are assumed to be consisted of two subsystems. Mass subsystem possesses low lateral stiffness but carries the major part of mass of the system. Stiffness subsystem, however, controls the deformation of the mass subsystem and attributes with much higher stiffness. In this study, for simplicity, stiffness subsystems are assumed to be rigid. Mass isolated systems are, therefore, striped down to

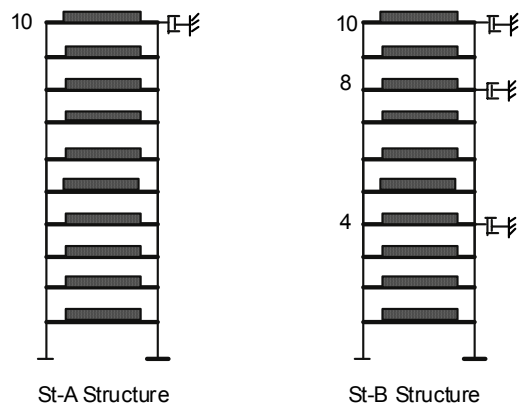mass subsystems supported laterally on dashpots.

Figure 3. Simplified Mass Isolated Structures

Both systems in Figure. 3 are, 10 storey structures with uniform mass and stiffness along the height. Shear stiffness of each storey is 56267 N/mm (inter-storey height is 3.0 meters) and mass of each floor is assumed to be at 200 N-Sec^2/mm. A proportional damping capacity (proportional to the stiffness) is also implanted into these systems to provide a damping ratio equivalent to 1% for the first mode in both systems. The first natural period of the above systems are 2.5 Sec. (before installing dashpots). St-A structure is equipped with a single dashpot at the top and St-B system possesses three identical dashpots at 4, 8 and 10 storey levels. Structures were analyzed subjecting to four well known earthquake records and spectrums (El-centro-S00E, Hachinohe-EW, Taft-EW and San-Fernando-S16). Figures. 4 and 5 are showing the response spectra of the above earthquakes for the two level of damping ratios (5% and 90%, respectively).
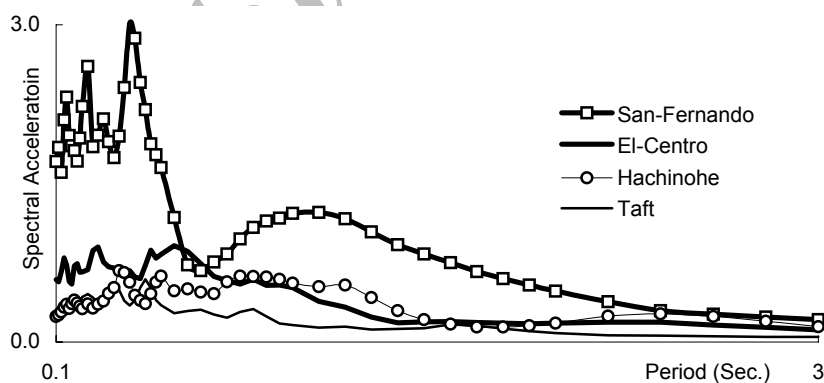
Figure 4. Earthquake spectrums for 5% damping ratio
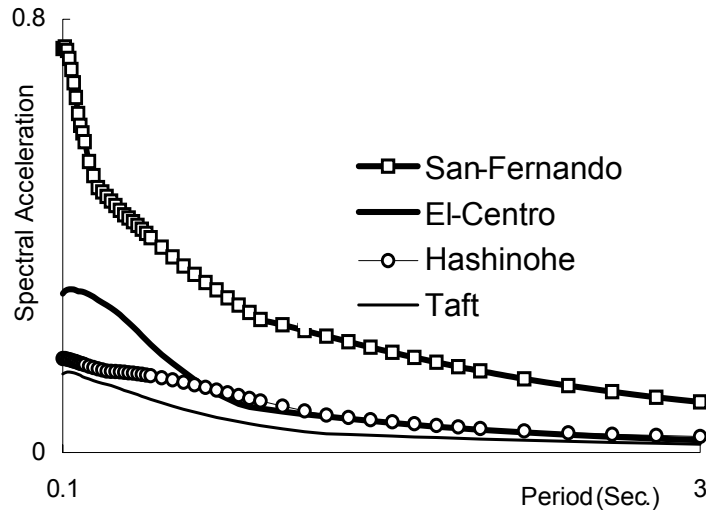
Figure 5. Earthquake spectrums for 90% damping ratio

5.1 System characteristics

Non-classical dynamic characteristics of the two systems (natural periods, modal shapes and damping ratios) for all the modes, considering different capacity of dashpots, are obtained using the state space approach ([5],[6] and [9]). Mass participation factors α_{NC}^{j} for all these cases are also computed using the proposed algorithm Eq. (24). System characteristics are tabulated in table 1 and 2 for St-A and St-B structures, respectively. In these tables C is the capacity of one dashpot alone and is determined, so as, damping ratio of the first mode of both structure to be adjusted to 5, 20, 40, 60 and 90 percents.
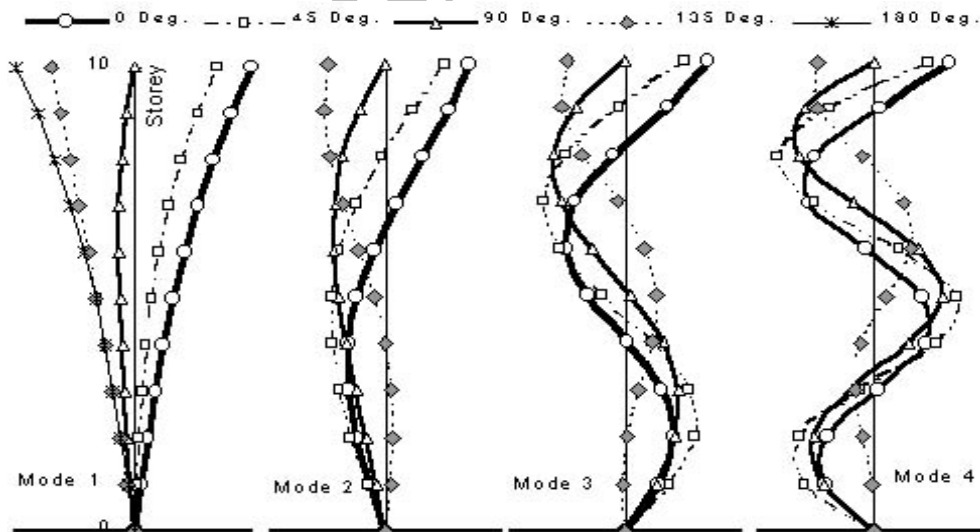
Figure 6. Modal Shapes of St-A structure at highest damping capacity (x1 =0.9)

Figure 6 represents the first 4 mode shapes of St-A structure when dashpot provides 90% damping ratio for the first mode of the system (C=3590 N-Sec/mm). Since modal shapes of non-classical systems consist of real and imaginary components, these components are combined in phase angles 0, 45, 90, 135 and 180 degrees and shown in the figure (phase angle 0 at the right side). Phase angles 0 and 90 degrees are respectively real and imaginary components of the mode shapes. In figure, combined resultants of some phase angles are eliminated for the sake of clarity.

According to the tables, increasing damping capacity results in decreasing the mass participation factor of the first mode (in the St-A structure, α_{NC}^1 has changed from 0.848 in low damping ratio to 0.755 for the highest damping ratio). On the other hand, this causes a substantial increase on MPF of the second mode (α_{NC}^2 in St-A system has reached to 0.186 from 0.091, more than twice). Comparing the characteristics of the two systems, St-B structure seems to be less affected by the change in damping capacity.

From the viewpoint of system characteristics, the above observations are quite valuable. Reducing mass participation factor of the first mode means cutting on that part of the mass of system that is actually transferred to the zone of low earthquake input energy. This may cause the possibility of higher modes domination and ineffectiveness of mass isolation. In St-A example the share of higher modes from total mass are increased from 15.2% (100%-84.8%) to 24.5%. Another point in here is the difference between St-A and St-B structures in system characteristics that shows the possibility of reducing non-classical features of the problem by distributing damping capacity along the height.

5.2 System characteristics vs. structural response
Reliability of the proposed definition for MPF can be verified through evaluation of the accuracy of base shear response of the structures using MPF definition in Eq. (31) or (25). Considering the concept of spectral approach in these relationships, at first, the role of system characteristics in estimation of base shear is determined. This phase of study requires a reference solution for the comparison purposes. In here, the same structure with classical characteristics is used as the bottom-line reference solution. In other words, two identical structures with classical and non-classical assumptions are compared in their system characteristics and modal base shear responses.

Assuming classical behavior, some of the system characteristics (periods and mass participation factors) will be equivalent to those of the original system with low damping capacity. Therefore, classical characteristics of the system are assumed to be similar to those reported in Table 1 (or Table 2) for the lowest damping ratio (5% for the first mode). Since in classical modal analysis damping ratios can not be mathematically obtained, in spectral analyses for the referenced classical system damping ratios originated from non-classical modal analyses (tabulated in Tables 1 and 2) are used to calculate the classical spectral base shear. Therefore, non-classical values of MPFs, periods and damping ratios are put into Eq. (31) to obtain non-classical spectral base shear (for each mode) and classical values of periods and MPFs along with non-classical damping ratios are used to calculate classical maximum modal base shear. Results of such comparisons between classical and non-classical systems are given, only, for St-A structure because of the domination of non-

classical behavior in this system.

Table 2. Non-Classical characteristics of **St-B** structure in terms of damping capacity of each dashpot

| Mode | Damping capacity (N-Sec/mm) | | | | | | | | | | | | | | |
| | C=100 | | | C=460 | | | C=935 | | | C=1400 | | | C=2050 | | |
	ξ	$T_{(Sec)}$	α_{NC}	ξ	$T_{(Sec)}$	α_{NC}	ξ	$T_{(Sec)}$	α_{NC}	ξ	$T_{(Sec)}$	α_{NC}	ξ	$T_{(Sec)}$	α_{NC}
1	0.05	2.51	0.848	0.20	2.50	0.847	0.40	2.48	0.846	0.60	2.45	0.841	0.90	2.38	0.831
2	0.046	0.84	0.091	0.095	0.84	0.091	0.158	0.84	0.092	0.22	0.84	0.095	0.31	0.85	0.102
3	0.058	0.51	0.031	0.07	0.51	0.032	0.089	0.51	0.033	0.10	0.51	0.035	0.12	0.51	0.038
4	0.081	0.37	0.014	0.10	0.37	0.014	0.136	0.37	0.014	0.17	0.37	0.013	0.22	0.37	0.013
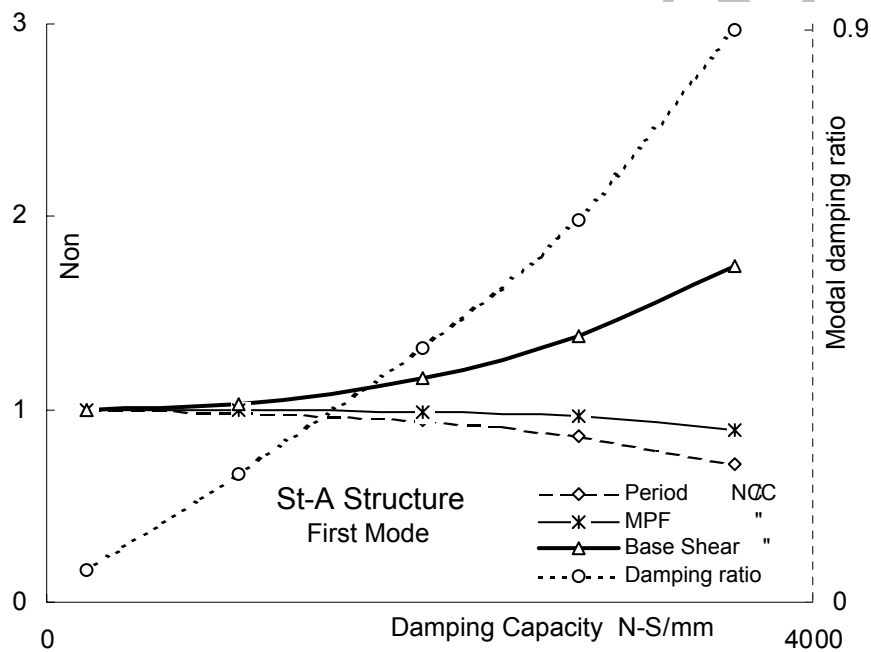
Figure 7. Non-classical to Classical ratios for the first mode of St-A structure

Figure 7 illustrates the ratio of non-classical to classical spectral base shear for the first mode of the system in terms of damping capacity in St-A structure. This ratio is based on average response of the system for all four earthquakes. The figure also shows the ratio of mass participation factor and natural period of the first mode of non-classical system to those of the classical one in terms of damping capacity. Moreover, the figure also represents the rate of change of damping ratio for the first mode of the structure with respect to damping capacity in the system (in right-side vertical axis). Similarly, Figures 8, 9 and 10 are showing the same type of relations for modes No. 2, 3 and 4, respectively.
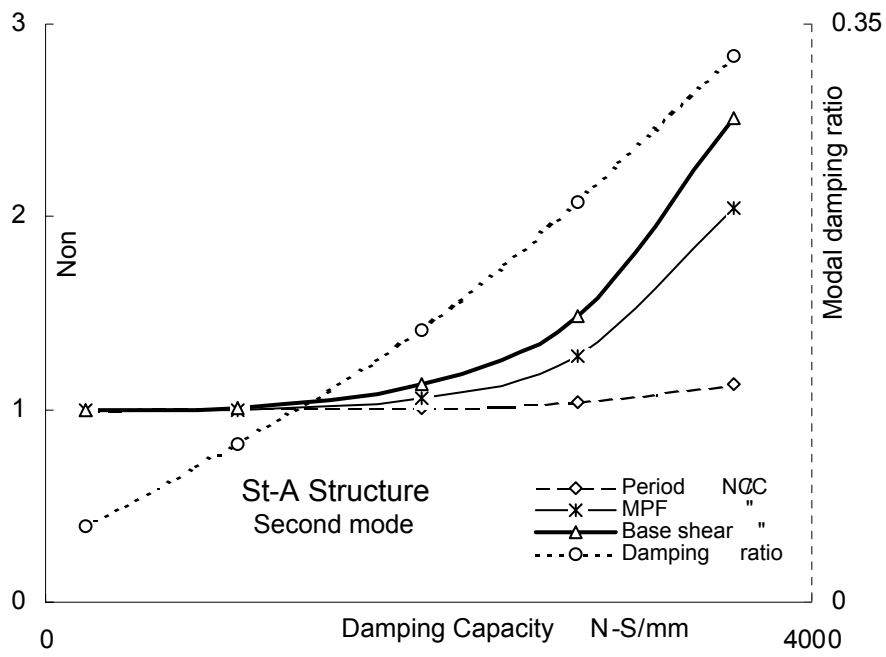
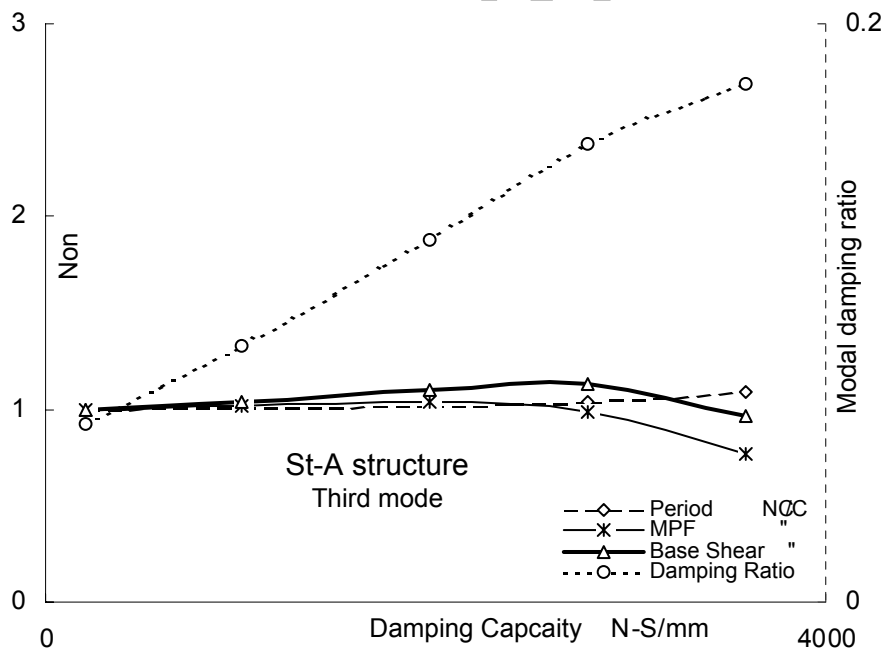Figure 8. Non-classical to Classical ratios for the second mode of St-A structure

Figure 9. Non-classical to Classical ratios for the third mode of St-A structure

As shown in figures, damping ratios are not linearly related to damping capacity in the system. In addition, figures also representing high ratios of non-classical base shear to the classical one (around 2 in highest damping capacities for most of the modes). This means the assumption of classical behavior for non-classical systems can be grossly misleading.

According to Figure 7, increasing damping capacity reduces the MPF but, unexpectedly, causes a substantial increase on the base shear ratio (i.e. lower MPF should cause lower base shear). However, increasing the base shear response in this case is attributed to the considerable change in the period of the first mode (from 2.5 Sec. down to 1.8 Sec.) that positioned the mode in high acceleration zone of the earthquakes spectrum. Nevertheless, as shown in Figures 8, 9 and 10, base shear in other modes is clearly affected by the rate of change of MPFs (considering unnoticeable changes in periods of these modes).

The above results indicate the importance of non-classical appraisal of system characteristics in determining spectral base shear for non-classical systems. More importantly, the results also indicate that, MPF definition in this study has a perceptible influence on base shear response of non-classical systems.

5.3 Spectral Modal base shear and MPF
Accuracy of the MPF definition for non-classical systems is still ambiguous. As described before, this ambiguity can be removed by evaluating the accuracy of spectral base shear response of the system. The reference solution in this verification is maximum value of the time history modal base shear (exact solution based on Eq. (20)). To have a bottom-line measure in determining the accuracy of non-classical spectral approach, again, spectral analyses for base shear using classical characteristics are performed.
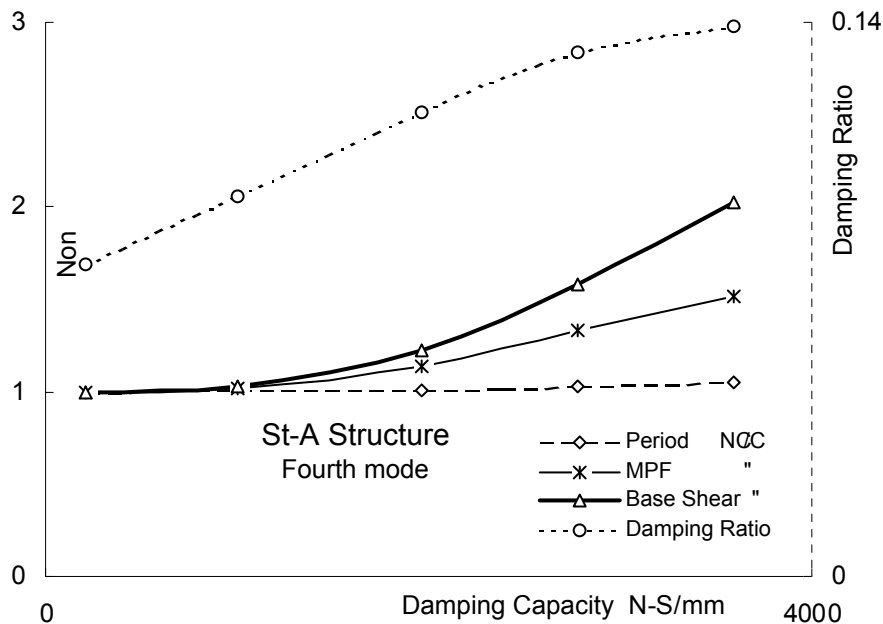

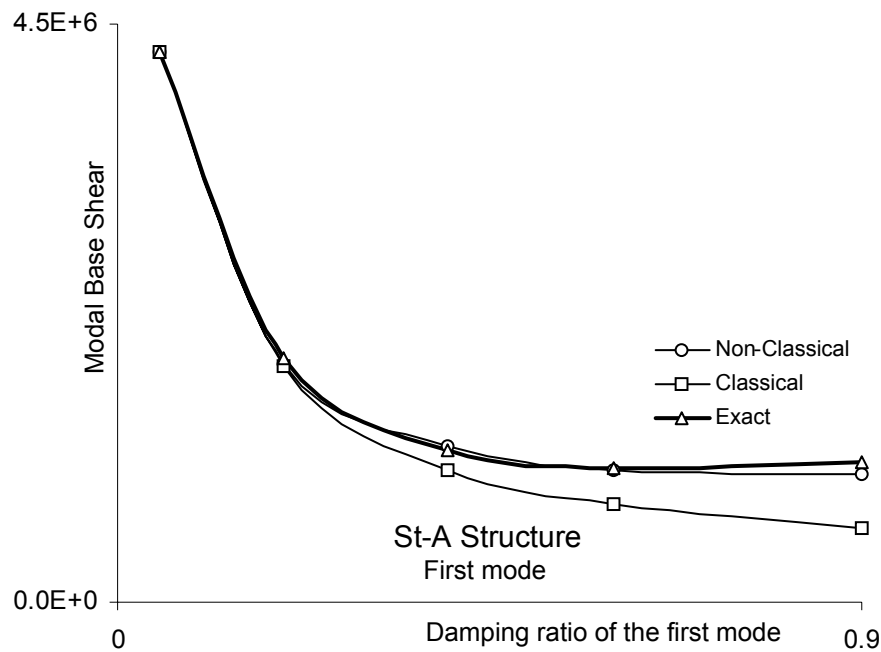Figure 10. Non-classical to Classical ratios for the fourth mode of St-A structure

Figure 11. Max. modal base shear of the first mode in St-A structure

Figure11 compares maximum base shear response of the first mode of the system, based on spectral (classical and non-classical) and time history analyses (in terms of damping ratio of the mode). The results are given for the St-A structure in the case of Hachinohe earthquake. Figures 12, 13 and 14 are illustrating the same features for modes No. 2, 3 and 4, respectively. To be able to compare the results of all modes, horizontal axes of these figures are scaled in terms of damping ratio of the first mode (the axes can be scaled back to damping ratio of each mode or dashpot capacity, C, using Table 1).

Table 1. Non-Classical characteristics of **St-A** structure in terms of damping capacity of dashpot

Mode	Damping capacity (N-Sec/mm)														
	C=206			C=1000			C=1965			C=2782			C=3590		
	ξ	$T_{(Sec)}$	α_{NC}	ξ	$T_{(Sec)}$	α_{NC}	ξ	$T_{(Sec)}$	α_{NC}	ξ	$T_{(Sec)}$	α_{NC}	ξ	$T_{(Sec)}$	α_{NC}
1	0.05	2.51	0.848	0.20	2.47	0.847	0.40	2.36	0.84	0.60	2.16	0.819	0.90	1.8	0.755
2	0.046	0.84	0.091	0.095	0.84	0.091	0.165	0.85	0.096	0.24	0.87	0.116	0.33	0.95	0.186
3	0.061	0.51	0.031	0.09	0.51	0.032	0.125	0.52	0.032	0.16	0.53	0.031	0.18	0.56	0.024

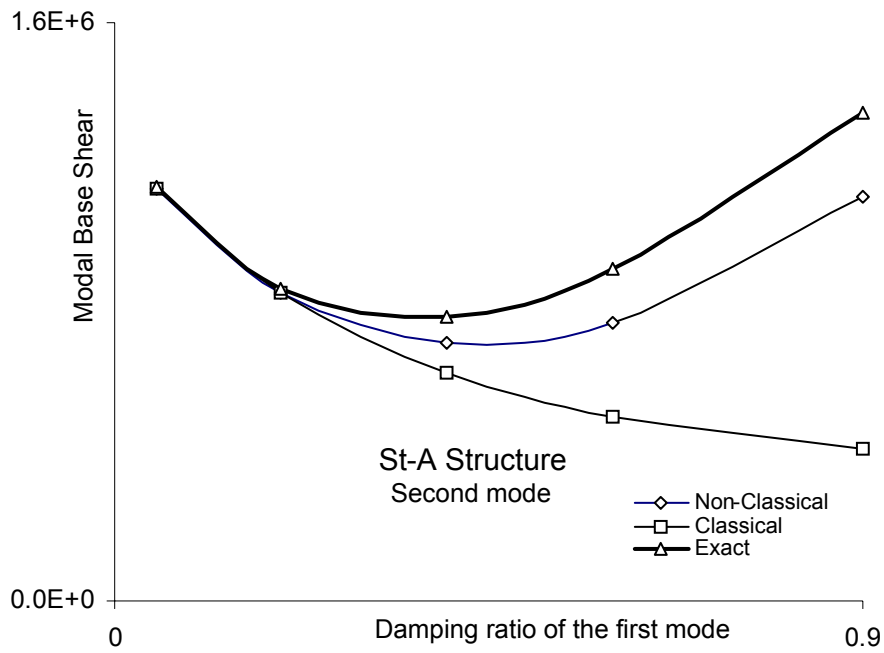| 4 | 0.079 | 0.37 | 0.014 | 0.01 | 0.38 | 0.014 | 0.117 | 0.38 | 0.016 | 0.13 | 0.39 | 0.019 | 0.14 | 0.39 | 0.022 |

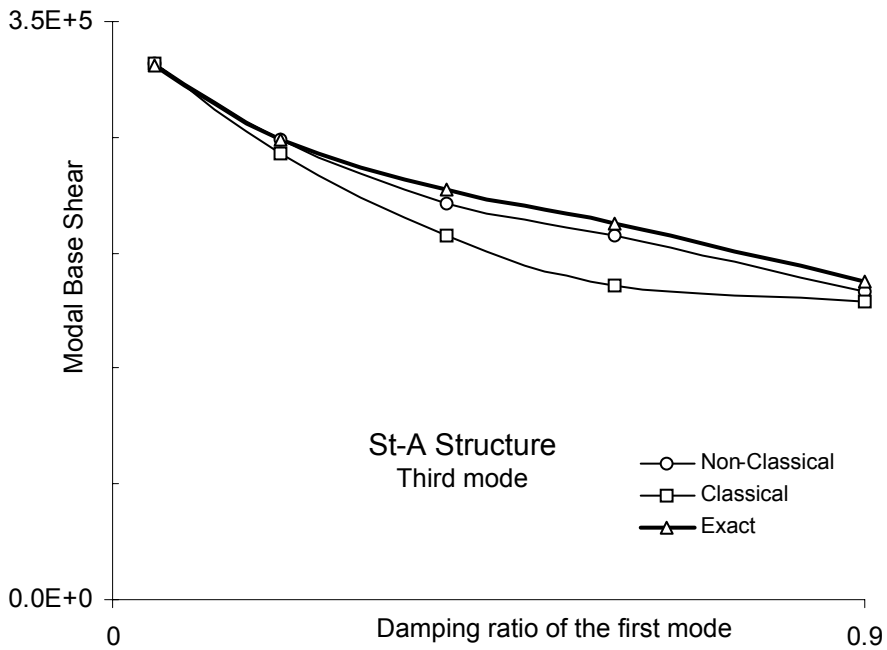Figure 12. Max. modal base shear of the second mode in St-A structure

Figure 13. Base shear response of the third mode in terms of damping ratio
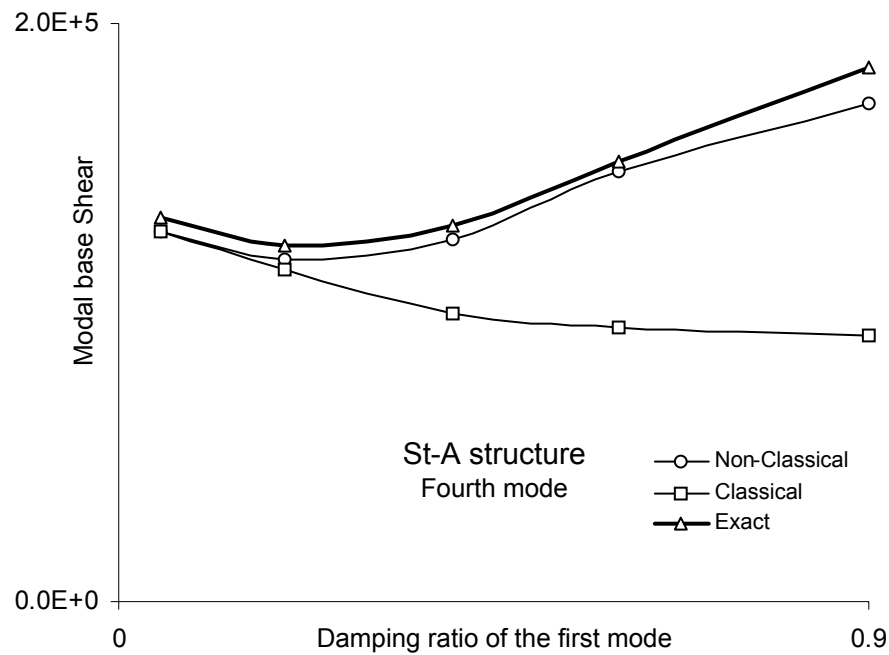

Figure 14. Base shear response of the fourth mode in terms of damping ratio

As shown in Figures. 11-14, there is a good agreement between non-classical spectral values of base shear and maximum values of time history response of the structure in all modes and in all range of damping ratios. However, classical spectral values for base shear are representing a trend that progressively underestimates base shear in all modes of the structure.

The same type of analysis has been carried out for other earthquake records (and spectrums) with basically the same results. Similarity of spectral non-classical modal base shear responses with those obtained by the time history analysis is a solid indication for accuracy of the proposed non-classical MPF (based on maximum values).

5.4 Time history response
As explained earlier, definition of Mass participation factor (MPF) in a classical system is not pending on maximum values and it comes directly from the time history relationship (i.e. Eq. (3)). Defining MPF based on maximum values would be more convincing if it shows its proximity to the time history definition. Eq. (30) presents the time history base shear response of the structure using the proposed MPF. This equation can not be a substitute for exact time history response of the system; however, it might be intriguing to see how it relates to the real time history base shear response of the structure.

A series of time history analyses using Eq. (18) and 30 for both St-A and St-B structures have been carried out. Damping capacities of structures are chosen the highest in this study (damping ratio of the first modes are 90%). Figure. 15 and 16 are showing time history base

shear responses of St-A structure subjected to two different earthquakes (El-Centro and Hachinohe). Note that, St-A structure with large damping capacity has the highest level of non-classical characteristics among all the examples (see Table 1).
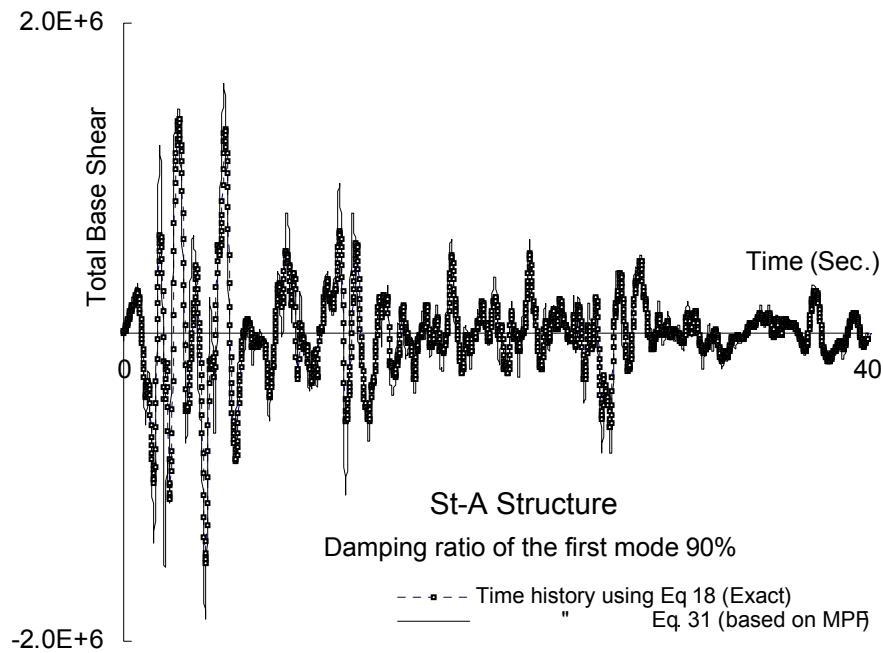

Figure 15. Time history total base shear for El-Centro earthquake
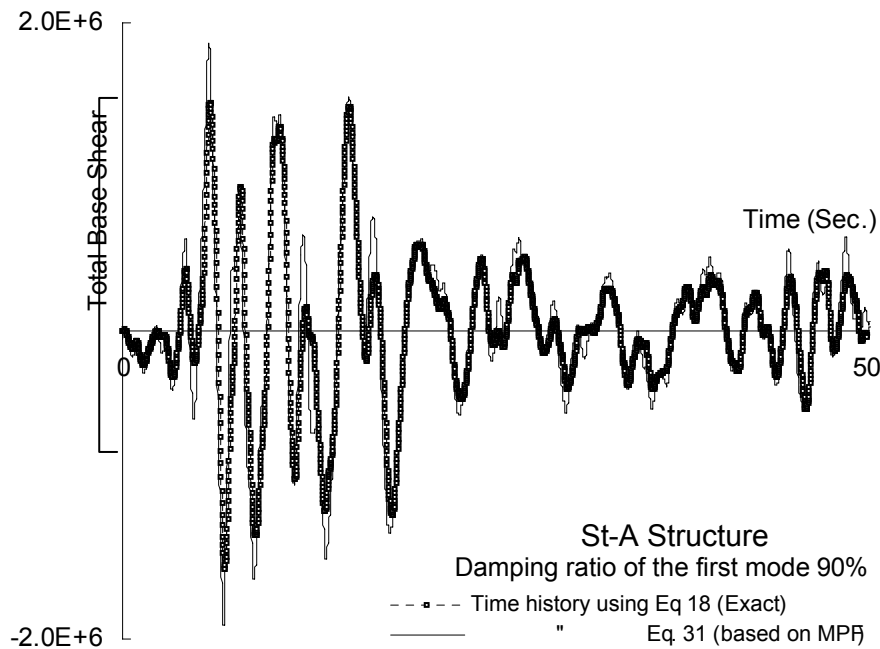
Figure 16. Time history total base shear for Hachinohe earthquake

As shown in figures, analyses based on Eq. (18) and 30 are not analogous responses in the time domain. However, Figure. 15 and 16 are representing plausible resemblance between the two relationships in depiction of time history base shear responses of the structure. Consequently, using the name Mass Participation Factor (MPF) for the parameter α_{NC}^{j} , derived based on maximum values, might be considered a viable designation.

It should be noted that, using MPF as a system characteristic in identification of mass isolation effectiveness requires less affinity to the concept of time history MPF due to the qualitative nature of system identification.

6. SPECTRAL ANALYSIS AND MODAL SUPERPOSITION

While the previous section was primarily dedicated to MPF verification, it was also contributed in supporting the proposed spectral analysis approach for maximum modal responses. However, reliability of the relationships for total responses (e.g. total base shear as indicated by Eq. (31)) may still need some more scrutiny due to the role of SRSS technique in modal superposition concept (see, Gupta [10] and Sinha et al. [15]).
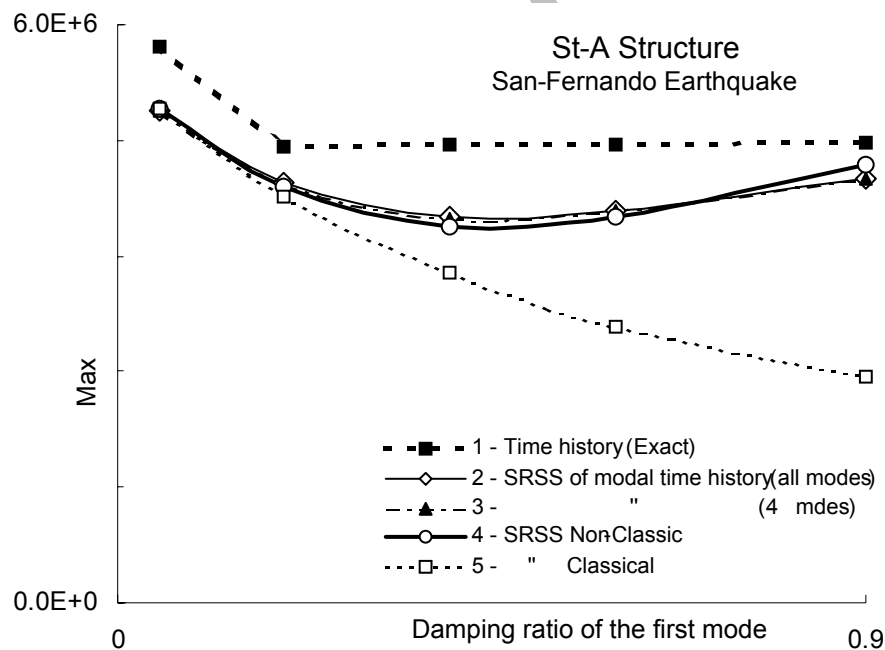

Figure 17. Max. Base shear in St-A structure subjected to San-Fernando earthquake

Figures. 17 and 18 are illustrating maximum total base shear response of the St-A structure subjected to San-Fernando and Hachinohe earthquakes. In these figures five

different approaches are shown in calculation of maximum base shear. The first one is based on time history analysis using all 10 modes of the system Eq. (18). This is considered the exact maximum value for total base shear. The second approach is to use time history analysis for all ten modes separately Eq. (20) and calculate the maximum total base shear using SRSS approach. The third analysis is the same as the second one but with the first four modes of the system (instead of 10 modes). The 4th approach uses Eq. (31) to find the maximum total base shear considering first four modes of the system (using the proposed MPF). The last technique is the so called classical spectral analysis (classical periods and mass participation factors but non-classical damping ratios) using first four modes of the system. As before, this analysis is provided for our bottom-line accuracy evaluation. Again, horizontal axes in these two figures are based on damping ratio of the first mode of the system.
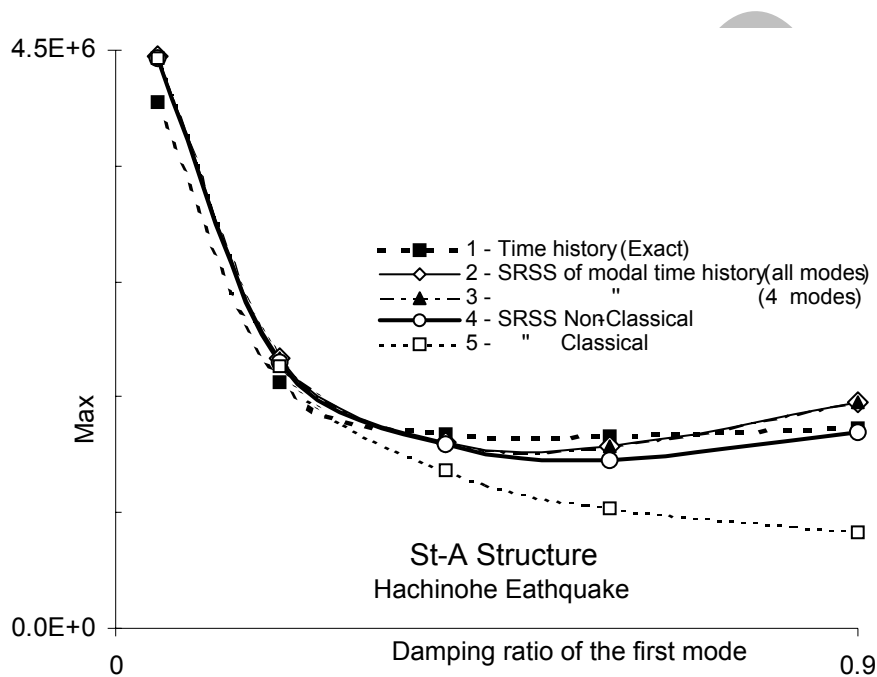

Figure 18. Max. Base shear in St-A structure subjected to Hachinohe Earthquake

As shown in figures, non-classical spectral approach (the 4th one) is quite accurate if it compares with the SRSS techniques for maximum modal time history responses (2nd and 3rd approaches). The classical spectral technique (5th method), however, is quite off the path in large damping ratios. Similarity between 3rd and 4th methods verifies the accuracy of our non-classical spectral approach and the MPF definition. Moreover, similarity between 2nd and 3rd methods indicates the marginal contribution of higher modes in total base shear response of the system.

Comparing all SRSS methods (2nd, 3rd and 4th except 5th) with the exact solution (1st approach) reveals the fact that, in San-Fernando earthquake SRSS technique is not accurate in providing a proper account for maximum total base shear (see, Figure. 17). On the

contrary, the same comparison for the case of Hachinohe earthquake represents indisputable accuracy of SRSS technique in estimating maximum base shear in all range of damping ratios (shown in Figure. 18). In other words, suitability of SRSS technique is not dependant on system characteristics alone and frequency content of earthquakes affects its accuracy. Moreover, since system characteristics in non-classical systems (natural periods and MPF) are dependent on the magnitude of damping capacity, accuracy of SRSS approach in such systems is not uniform across a wide range of change in damping ratios (as shown in Figure. 17).
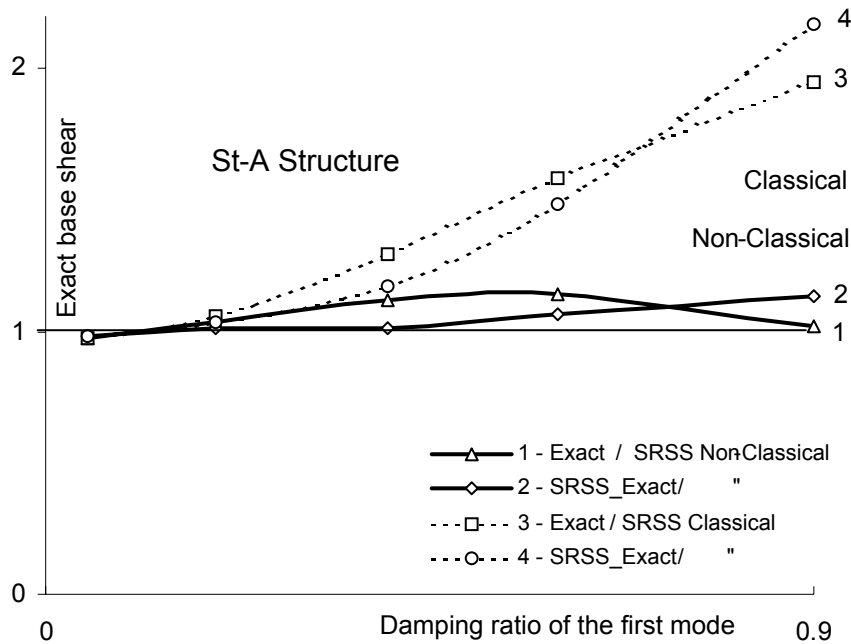

Figure 19. Average ratios of exact base shear to SRSS approachs for all Earthquakes

Figure 19 shows average (four earthquakes) ratio of exact maximum base shear of the St-A structure (1st approach) to its SRSS appraisal of non-classical spectral counterpart (4th approach). The figure also shows the average ratio of SRSS evaluation of base shear using exact maximum modal values (3rd approach) to that of the SRSS spectral method (4th approach, again). Curves No. 1 and 2 are respectively depicting these parameters in terms of damping ratio of the fist mode. The same ratios in terms of classical spectral analysis (5th approach instead of 4th) are also shown in the figure (curves 3 and 4) to compare the consistency of MPF definition in classical and non-classical approaches.

Considering the close distance between curves 1 and 2 in Figure.19, accuracy of non-classical spectral analysis (that uses MPF) seems to be at the same level of accuracy of SRSS approach in dealing with exact modal base shear. According to the figure, the same level of proximity between curves No. 1 and 2 also exist between curves 3 and 4. Thus, no matter what kind of spectral analysis (classical or non-classical) or even SRSS of exact maximum modal values are used; accuracy of total response is dominated, mostly, by the suitability of SRSS

technique in superposing modal effects. This conclusion may help to justify the appropriateness of non-classical spectral analysis and the MPF definition in this study.
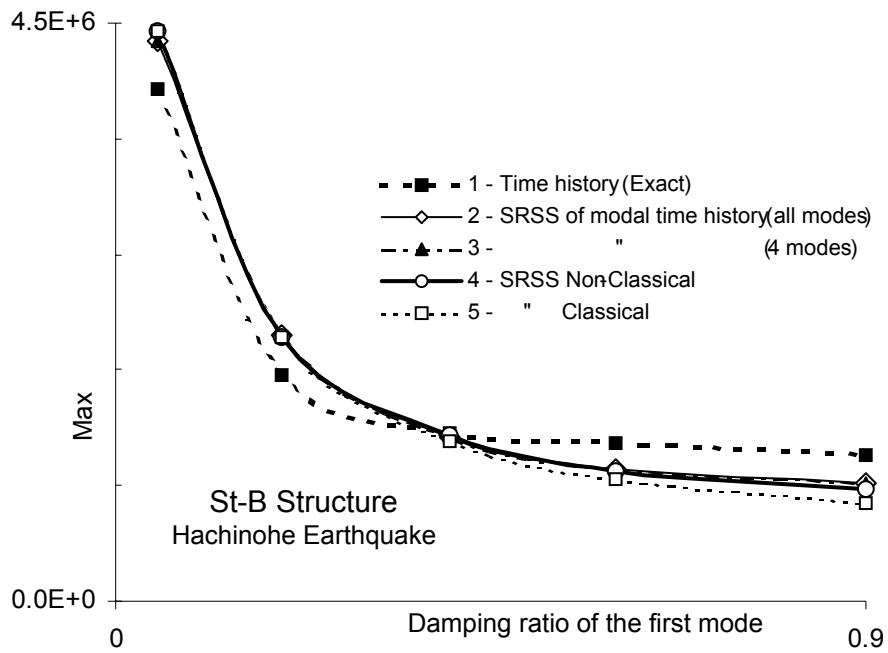

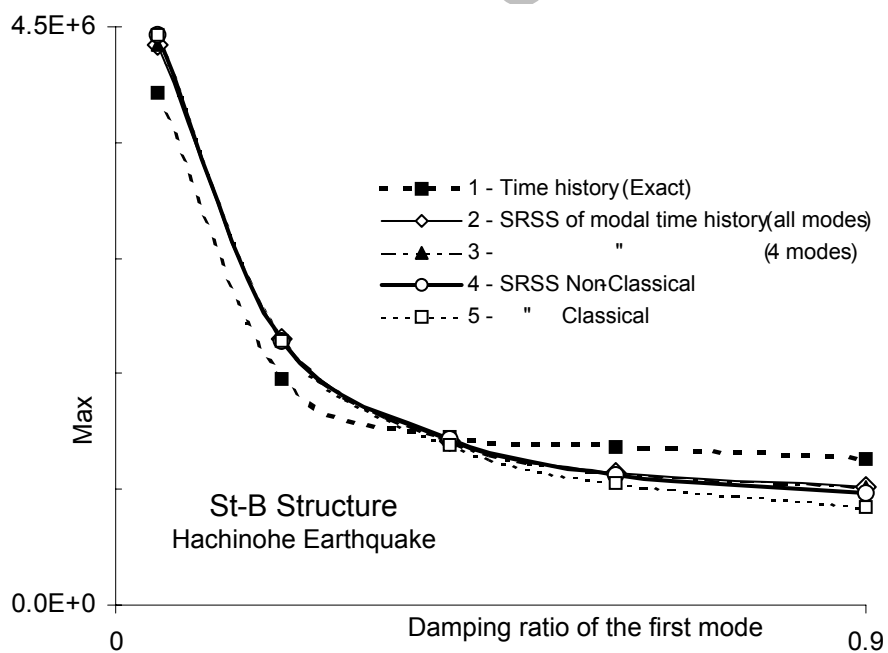Figure 20. Max. Base shear in ST-B structure subjected to San-Fernando earthquake

Figure 21. Max. Base shear in ST-B structure subjected to Hachinohe earthquake

7. MASS ISOLATION AND DAMPING CAPACITY DISTRIBUTION

Referring to our earlier discussion, distribution of damping capacity in structures substantially reduces the non-classical aspects of the system. This was shown by the system characteristics (periods and MPFs) of St-A and St-B structures tabulated in table 1 and 2. Moreover, the results of analyses for base shear response of the same structures demonstrate the significance of this issue in designing mass isolated systems.

Analogous to Figures. 17 and 18 for St-A structure, maximum total base shear responses of St-B system subjected to San-Fernando and Hachinohe earthquakes are shown in Figure. 20 and 21, respectively. Comparing the results, two important points in designing of such systems are revealed. First, in high damping ratios, distribution of damping capacity in structures reduces the level of structural response in the system (around 30% reduction in total base shear at highest damping ratio). More importantly, as shown in Figures. 20 and 21, the threshold of splitting classical and non-classical solutions in St-B structure starts at much higher damping ratios (comparing with that of St-A structure shown in Figures.17 and 18). According to these figures, if damping ratio of 20% in St-A structure is the threshold of non-classical behavior for base shear response of the system, in St-B structure this ratio is around 60%. Note that, for other responses of the system (e.g. lateral force distribution along the height) these ratios could be quite different.

Consequently, in designing mass isolated systems distribution of damping capacity along the height reduces the structural response of the system and provides the ground for classical analytical tools to be applicable in higher range of damping ratios.

8. CONCLUSIONS

Mass participation factor (MPF) as a system characteristic is an important parameter in identification of mass isolated systems and speculation on their effectiveness in reducing earthquake effects on structures. In this study a methodology for calculating mass participation factor for non-classical mass isolated systems is proposed. In contrast with classical systems, MPF definition in this approach is based on maximum value of modal base shear. Accuracy of the proposed MPF is verified through some numerical examples. According to these results increasing damping capacity in non-classical systems may reduce the contribution of the first mode in response of the structure in expenses of increasing the share of higher modes in the system. Afterward, by expanding the same approach in deriving MPF, a spectral analysis technique for non-classical system is proposed that possesses both simplicity and accuracy in the analysis procedure. Applicability of classical analytical tools in determining the behavior of mass isolated systems is also examined. It is shown that, distribution of damping capacity in the structure will reduce the non-classical features of the problem and extends the possibility of using classical analytical tools in studying the behavior of such systems.

REFERENCES

1. Skinner, R.I., Robinson, W.H. and McVerry G.H. *An Introduction to Seismic Isolation*. John Wiley & Sons: New York, 1993.

2. Ziyaeifar, M. and Noguchi, H. Partial Mass Isolation in tall buildings. *Journal of Earthquake Engineering and Structural Dynamics*, **27**(1998) 49-65.

3. Ziyaeifar, M. Mass isolation, concept and techniques. *European Earthquake Engineering*. **2**(2002) 64-76.

4. Naeim, F. and Kelly, J.M. *Design of seismic isolated structures: from theory to practice*. John Wiley & Sons: New York, 1999.

5. Foss, K.A. Co-ordinates which uncouple the equations of motion of damped linear dynamic systems. *J. Appl. Mech*. ASME, **25**(1958) 361-364.

6. Argyris, J. Melejnek, H.P. *Dynamics of Structures*. Elsevier Science Publishers: Amsterdam, The Netherlands,1991.

7. Caughey, T.K. and O'kelly M.E.J. Classical Normal Modes in Damped Linear Dynamic Systems. *J. Appl. Mech*. ASME, **32**(1965) 583-588.

8. Clough, R.W. Penzien J. *Dynamics of Structures*. McGraw-Hill: New York, NY, 1993.

9. Veletsos, A.S, Ventura CE. Modal analysis of non-classical damped linear systems. *Earthquake Eng*. Struct. Dyn. **14**(1986) 217-243.

10. Gupta, A.K. *Response spectrum method in seismic analysis and design of structures*. Blackwell Scientific: Cambridge, Mass., 1990.

11. Igusa, T. Der Kiureghian, A. and Sackman, J.L. Modal decomposition method for stationary response of non-classically damped systems. *Earthquake Eng. Struct. Dyn.* **12(**1984) 121-136.

12. Pekcan, G. Mander, J.B. and Chen, S.S. Fundamental considerations for the design of non-linear viscous dampers. *Earthquake Eng. Struct. Dyn.* **28**(1999) 1405-1425.

13. Der Kiureghian, A. A response spectrum method for random vibration analysis of MDF systems. *Earthquake Eng. Struct. Dyn.* **9**(1981) 419-435.

14. Villaverde, R. Newmark NM. Seismic Response of light attachments to buildings. *SRS No. 469*. University of Illinois: Urbana, 1980.

15. Sinha, R. and Igusa, T. CQC and SRSS methods for non-classically damped structures. *Earthquake Eng. Struct. Dyn.* **24**(1995) 615-619.